Journal of Statistical Physics, Vol. 112, Nos. 3/4, August 2003 (© 2003)

Nonlinear Transport in Inelastic Maxwell Mixtures Under Simple Shear Flow

Vicente Garzó[1]

Received November 18, 2002; accepted February 20, 2003

The Boltzmann equation for inelastic Maxwell models is used to analyze nonlinear transport in a granular binary mixture in the steady simple shear flow. Two different transport processes are studied. First, the rheological properties (shear and normal stresses) are obtained by solving exactly the velocity moment equations. Second, the diffusion tensor of impurities immersed in a sheared inelastic Maxwell gas is explicitly determined from a perturbation solution through first order in the concentration gradient. The corresponding reference state of this expansion corresponds to the solution derived in the (pure) shear flow problem. All these transport coefficients are given in terms of the restitution coefficients and the parameters of the mixture (ratios of masses, concentration, and sizes). The results are compared with those obtained analytically for inelastic hard spheres in the first Sonine approximation and by means of Monte Carlo simulations. The comparison between the results obtained for both interaction models shows a good agreement over a wide range values of the parameter space.

KEY WORDS: Nonlinear transport; granular mixtures; inelastic Maxwell models; Boltzmann equation.

1. INTRODUCTION

Granular media under rapid flow conditions are usually modeled by a fluid of hard spheres with inelastic collisions. In the simplest version, the grains are taken to be smooth so that the inelasticity is only characterized through a constant coefficient of normal restitution. For a low-density gas, the Boltzmann equation has been conveniently generalized[1] to account for the inelasticity of binary collisions and the Navier–Stokes transport coefficients

[1] Departamento de Física, Universidad de Extremadura, E-06071 Badajoz, Spain; e-mail: vicenteg@unex.es

0022-4715/03/0800-0657/0 © 2003 Plenum Publishing Corporation

have been obtained in terms of the restitution coefficient.[2–5] As in the case of elastic collisions, these transport coefficients verify a set of coupled linear integral equations which are solved approximately by using the leading terms in a Sonine polynomial expansion. The corresponding Sonine results are in general in good agreement with selected tests using molecular dynamics[6] and Monte Carlo simulations.[4, 7, 8] However, beyond the Navier–Stokes regime (small spatial hydrodynamic gradients), it is quite intricate to get explicit results for inelastic hard spheres (IHS) and one has to resort to alternative approaches.

One of the main mathematical difficulties in solving the Boltzmann equation for hard spheres (even in the elastic case) comes from the form of the collision rate, which is proportional to the magnitude of the relative velocity of the two colliding spheres. In the case of elastic fluids, a possible way to overcome this problem is to assume that the particles interact via the repulsive Maxwell potential (inversely proportional to the fourth power of the distance). For this interaction model, the collision rate is independent of the relative velocity and this allows for a number of nice mathematical properties of the Boltzmann collision operator.[9] Thanks to this simplification, nonlinear transport properties can be exactly obtained[10–12] from the Boltzmann equation for Maxwell elastic molecules and, when properly reduced, they exhibit a good agreement with results obtained for other interaction models.[13] In the context of inelastic gases, the Boltzmann equation for inelastic Maxwell models (IMM) was also introduced about two years ago.[14–16] The IMM share with elastic Maxwell molecules the property that the collision rate is velocity independent but their collision rules are the same as for IHS. As a consequence, these IMM's do not describe real particles since they do not interact according to a given potential law. For this reason the model is usually referred to as pseudo-Maxwellian model.[15] Nevertheless, the IMM keeps the qualitatively correct structure and properties of the nonlinear macroscopic equations and obey Haff's law.[17]

The Boltzmann equation for IMM has received a great attention in the last few years, especially in the study of overpopulated high energy tails in homogeneous states.[17–22] The existence of high energy tails of the Boltzmann equation is common for IHS and IMM, although this general qualitative agreement fails at a quantitative level. For inhomogeneous states, the Chapman–Enskog method has been recently applied to the Boltzmann equation to get the Navier–Stokes transport coefficients.[23, 24] The comparison with the results derived for the IHS model[2] shows in general significant discrepancies in the dependence of the transport coefficients on the restitution coefficient. On the other hand, the results obtained here for a quite different state show close agreement between the IMM and IHS. The

IMM has been also used to get the shearing stress of a granular material under shear flow.[25] All the above results refer to monocomponent gases. Much less is known for inelastic Maxwell mixtures. In the case of multicomponent gases, Marconi and Puglisi[26] have analyzed energy nonequipartition in the free cooling and driven states for a one-dimensional system, while Ben-Naim and Krapivsky[27] have studied velocity statistics of an impurity inmersed in a uniform granular fluid. However, to the best of my knowledge, no previous study on transport properties in inelastic Maxwell mixtures has been carried out.

The aim of this paper is to analyze nonlinear transport in a binary mixture in the framework of the Boltzmann equation for IMM. Two different transport processes will be studied. First, the rheological properties (shear stress and normal stress differences) of a granular binary mixture subjected to the simple shear flow will be explicitly determined. Second, the elements of the tracer diffusion tensor characterizing the diffusion of impurities in a granular gas under shear flow will be obtained in the first order of the concentration gradient. In both situations, given the coupling between dissipation and the shear rate, the mixture is far away from equilibrium and the Navier–Stokes constitutive equations[2, 4, 23, 24] do not apply. This makes the analytical treatment of both nonequilibrium situations difficult. An additional complication arises from the large number of parameters governing the dynamics of the system, including three independent restitution coefficients. However, the tractability of the Boltzmann collision integrals for IMM allows one to determine all the above nonlinear transport properties by solving exactly the hierarchy of moment equations. The results derived for IMM are then compared with those recently obtained for IHS in the leading Sonine approximation[28, 29] and by means of Monte Carlo simulations.[28, 30] Since the strength of the shear rate is arbitrary the test of the capability of IMM to capture the relevant behavior of IHS is quite stringent. The comparison performed here shows that in general the agreement between both interaction models is quite good, even for strong dissipation. This fact increases the degree of reliability of IMM as a physical model to describe transport properties of granular media under rapid flow conditions and is perhaps one of the most surprising results reported in this paper.

The plan of the paper is as follows. In Section 2 the Boltzmann equation for IMM and the macroscopic conservation laws are introduced. Section 3 deals with the simple shear flow problem for inelastic Maxwell mixtures. The elements of the pressure tensor are exactly obtained in terms of the restitution coefficients and the parameters of the mixture (masses, sizes, and concentrations). In particular, the results show that both species have different temperatures so that the energy is not equally distributed

between both species (breakdown of energy equipartition). The diffusion tensor of impurities in a Maxwellian sheared fluid is obtained in Section 4. The paper is closed in Section 5 with some concluding remarks.

2. THE BOLTZMANN EQUATION AND THE INELASTIC MAXWELL MODEL

Let us consider a binary mixture of inelastic Maxwell gases at low density. In the simplest version, the Boltzmann equation for IMM[14, 17, 20, 23, 27] can be obtained from the Boltzmann equation for IHS by replacing the rate for collisions between particles of species r and s by an average velocity-independent collision rate, which is proportional to the square root of the temperature. This means that a random pair of colliding particles undergo inelastic collisions with a random impact direction. With this simplification, the set of nonlinear Boltzmann kinetic equations become

$$\left(\frac{\partial}{\partial t}+\mathbf{v}_1\cdot\nabla\right) f_r(\mathbf{r},\mathbf{v}_1;t)=\sum_s J_{rs}[\mathbf{v}_1\mid f_r(t), f_s(t)], \tag{1}$$

where $f_r(\mathbf{r},\mathbf{v}_1;t)$ is the one-particle distribution function of species r ($r=1,2$) and the Boltzmann collision operator $J_{rs}[\mathbf{v}_1\mid f_r, f_s]$ describing the scattering of pairs of particles is

$$J_{rs}[\mathbf{v}_1\mid f_r, f_s] = \frac{w_{rs}}{n_s\Omega_d}\int d\mathbf{v}_2\int d\hat{\boldsymbol{\sigma}}[\alpha_{rs}^{-1} f_r(\mathbf{r},\mathbf{v}_1',t)\, f_s(\mathbf{r},\mathbf{v}_2',t)-f_r(\mathbf{r},\mathbf{v}_1,t)\, f_s(\mathbf{r},\mathbf{v}_2,t)]. \tag{2}$$

Here, n_s is the number density of species s, w_{rs} is an effective collision frequency (to be chosen later) for collisions of type $r-s$, $\Omega_d=2\pi^{d/2}/\Gamma(d/2)$ is the total solid angle in d dimensions, and $\alpha_{rs}\leqslant 1$ refers to the constant restitution coefficient for collisions between particles of species r with s. In addition, the primes on the velocities denote the initial values $\{\mathbf{v}_1',\mathbf{v}_2'\}$ that lead to $\{\mathbf{v}_1,\mathbf{v}_2\}$ following a binary collision:

$$\mathbf{v}_1'=\mathbf{v}_1-\mu_{sr}(1+\alpha_{rs}^{-1})(\hat{\boldsymbol{\sigma}}\cdot\mathbf{g}_{12})\,\hat{\boldsymbol{\sigma}},\qquad \mathbf{v}_2'=\mathbf{v}_2+\mu_{rs}(1+\alpha_{rs}^{-1})(\hat{\boldsymbol{\sigma}}\cdot\mathbf{g}_{12})\,\hat{\boldsymbol{\sigma}}, \tag{3}$$

where $\mathbf{g}_{12}=\mathbf{v}_1-\mathbf{v}_2$ is the relative velocity of the colliding pair, $\hat{\boldsymbol{\sigma}}$ is a unit vector directed along the centers of the two colliding spheres, and

$$\mu_{rs}=\frac{m_r}{m_r+m_s}. \tag{4}$$

There is another more refined version of the inelastic Maxwell model[15, 16, 31] where the collision rate has the same dependence on the scalar product $(\hat{\boldsymbol{\sigma}}\cdot\hat{\mathbf{g}}_{12})$ as in the case of hard spheres. The corresponding Boltzmann equation can be proved to be equivalent to Eq. (1) except that the collision laws (3) must be changed. However, both versions of IMM lead to similar results in problems as delicate as the high energy tails.[17] Therefore, for the sake of simplicity, here I will consider the version given by the collision rules (3). As will be shown later, this model compares quite well with the results obtained from the IHS model.

At a hydrodynamic level, the relevant quantities in a binary mixture are the number densities n_r, the flow velocity $\mathbf{u}$, and the "granular" temperature T. They are defined in terms of moments of the distribution f_r as

$$n_r = \int d\mathbf{v}\, f_r(\mathbf{v}), \qquad \rho\mathbf{u} = \sum_r \rho_r \mathbf{u}_r = \sum_r \int d\mathbf{v}\, m_r \mathbf{v} f_r(\mathbf{v}), \tag{5}$$

$$nT = \sum_r n_r T_r = \sum_r \int d\mathbf{v}\, \frac{m_r}{d} V^2 f_r(\mathbf{v}), \tag{6}$$

where $\rho_r = m_r n_r$, $n = n_1 + n_2$ is the total number density, $\rho = \rho_1 + \rho_2$ is the total mass density, and $\mathbf{V} = \mathbf{v} - \mathbf{u}$ is the peculiar velocity. Equations (5) and (6) also define the flow velocity $\mathbf{u}_r$ and the partial temperature T_r of species r, the latter measuring the mean kinetic energy of species r.

The collision frequencies w_{rs} can be seen as free parameters in the model. Its dependence on the restitution coefficients α_{rs} can be chosen to optimize the agreement with the results obtained from the Boltzmann equation for IHS. Of course, the choice is not unique and may depend on the property of interest.

The collision operators conserve the particle number of each species and the total momentum, but the total energy is not conserved. This implies that

$$\sum_{r,s} \int d\mathbf{v}\, \frac{1}{2} m_r V^2 J_{rs}[\mathbf{v} \mid f_r, f_s] = -\frac{d}{2} nT\zeta, \tag{7}$$

where ζ is identified as the "cooling rate" due to inelastic collisions among all species. At a kinetic level, it is also convenient to discuss energy transfer in terms of the "cooling rates" ζ_r for the partial temperatures T_r. They are defined as

$$\zeta_r = \sum_s \zeta_{rs}, \tag{8}$$

where

$$\zeta_{rs} = -\frac{1}{dn_r T_r} \int d\mathbf{v}\, m_r V^2 J_{rs}[\mathbf{v} \mid f_r, f_s]. \tag{9}$$

The total cooling rate ζ can be expressed in terms of the partial cooling rates ζ_r as

$$\zeta = T^{-1} \sum_r x_r T_r \zeta_r, \tag{10}$$

where $x_r = n_r/n$ is the mole fraction of species r.

The macroscopic balance equations follow from the Boltzmann equations (1) by taking velocity moments. They are given by

$$D_t n_r + n_r \nabla \cdot \mathbf{u} + \frac{\nabla \cdot \mathbf{j}_r}{m_r} = 0, \tag{11}$$

$$D_t \mathbf{u} + \rho^{-1} \nabla \mathsf{P} = 0, \tag{12}$$

$$D_t T - \frac{T}{n} \sum_r \frac{\nabla \cdot \mathbf{j}_r}{m_r} + \frac{2}{dn} (\nabla \cdot \mathbf{q} + \mathsf{P} : \nabla \mathbf{u}) = -\zeta T. \tag{13}$$

In the above equations, $D_t = \partial_t + \mathbf{u} \cdot \nabla$ is the material derivative,

$$\mathbf{j}_r = m_r \int d\mathbf{v}\, \mathbf{V} f_r(\mathbf{v}) \tag{14}$$

is the mass flux for species r relative to the local flow,

$$\mathsf{P} = \sum_r \int d\mathbf{v}\, m_r \mathbf{V}\mathbf{V} f_r(\mathbf{v}) \tag{15}$$

is the total pressure tensor, and

$$\mathbf{q} = \sum_r \int d\mathbf{v}\, \tfrac{1}{2} m_r V^2 \mathbf{V} f_r(\mathbf{v}) \tag{16}$$

is the total heat flux.

The main advantage of using IMM is that a velocity moment of order k of the Boltzmann collision operator only involves moments of order less than or equal to k.[12, 31] This allows one to determine the Boltzmann collision moments without the explicit knowledge of the velocity distribution function. In general, beyond the linear hydrodynamic regime (Navier–Stokes order), the above property is not sufficient to exactly solve the

hierarchy of moment equations due to the free-streaming term of the Boltzmann equation. Nevertheless, there exist some particular situations (such as the simple shear flow problem) for which the above hierarchy can be recursively solved. The first few moments of the Boltzmann collision operator $J_{rs}[f_r, f_s]$ have been evaluated in Appendix A. They can be written as

$$\int d\mathbf{v}\, m_r \mathbf{V} J_{rs}[f_r, f_s] = -\frac{w_{rs}}{\rho_s d}\mu_{sr}(1+\alpha_{rs})(\rho_s \mathbf{j}_r - \rho_r \mathbf{j}_s), \tag{17}$$

$$\begin{aligned}\int d\mathbf{v}\, m_r \mathbf{V}\mathbf{V} J_{rs}[f_r, f_s] = -\frac{w_{rs}}{\rho_s d}\mu_{sr}(1+\alpha_{rs})\Big\{ & 2\rho_s \mathsf{P}_r - (\mathbf{j}_r \mathbf{j}_s + \mathbf{j}_s \mathbf{j}_r) \\ & -\frac{2}{d+2}\mu_{sr}(1+\alpha_{rs})\Big[\rho_s \mathsf{P}_r + \rho_r \mathsf{P}_s - (\mathbf{j}_r \mathbf{j}_s + \mathbf{j}_s \mathbf{j}_r) \\ & +\Big[\frac{d}{2}(\rho_r p_s + \rho_s p_r) - \mathbf{j}_r \cdot \mathbf{j}_s\Big]\mathbb{1}\Big]\Big\},\end{aligned} \tag{18}$$

where

$$\mathsf{P}_r = \int d\mathbf{v}\, m_r \mathbf{V}\mathbf{V} f_r, \tag{19}$$

$p_r = n_r T_r = \operatorname{tr} \mathsf{P}_r / d$ is the partial pressure of species r, and $\mathbb{1}$ is the $d \times d$ unit tensor. The relationship between the collision frequency w_{rs} and the cooling rate ζ_{rs} can be obtained by taking the trace in Eq. (18):

$$\zeta_{rs} = \frac{2w_{rs}}{d}\mu_{sr}(1+\alpha_{rs})\Big[1 - \frac{\mu_{sr}}{2}(1+\alpha_{rs})\frac{\theta_r + \theta_s}{\theta_s} + \frac{\mu_{sr}(1+\alpha_{rs})-1}{d\rho_s p_r}\mathbf{j}_r \cdot \mathbf{j}_s\Big], \tag{20}$$

where

$$\theta_1 = \frac{1 + x_1(\gamma - 1)}{\mu_{21}\gamma}, \qquad \theta_2 = \frac{1 + x_1(\gamma - 1)}{\mu_{12}}, \tag{21}$$

and $\gamma \equiv T_1/T_2$ is the temperature ratio.

3. RHEOLOGICAL PROPERTIES UNDER SIMPLE SHEAR FLOW

As said in the Introduction, one of the main objectives of the present paper is to evaluate the rheological properties of an inelastic Maxwell binary mixture subjected to the simple shear flow. At a macroscopic level,

this state is characterized by a constant linear velocity profile $\mathbf{u} = \mathbf{u}_1 = \mathbf{u}_2 = \mathsf{a} \cdot \mathbf{r}$, where the elements of the tensor a are $a_{ij} = a\delta_{ix}\delta_{jy}$, a being the constant shear rate. In addition, the partial densities n_i and the granular temperature T are uniform, while the mass and heat fluxes vanish by symmetry reasons ($\mathbf{j}_r = \mathbf{q} = \mathbf{0}$). As a consequence, the (uniform) pressure tensor P is the only nonzero flux in the problem. On the other hand, according to the energy balance equation (13), the temporal variation of the granular temperature arises from the balance of two opposite effects: viscous heating and collisional cooling. When both mechanisms cancel each other, a steady state is achieved and the temperature remains constant. In that case, the shear stress P_{xy} and the cooling rate ζ are related by

$$aP_{xy} = -\frac{d}{2}\zeta p, \tag{22}$$

where $p = \text{tr}\,\mathsf{P}/d = nT$ is the pressure. My goal here is to determine the pressure tensor P in this steady state.

The simple shear flow becomes spatially uniform when one refers the velocities of the particles to a frame moving with the flow velocity $\mathbf{u}$: $f_s(\mathbf{r}, \mathbf{v}) \to f_s(\mathbf{V})$. Consequently, the corresponding steady Boltzmann equations (1) read

$$-a_{ij}V_j \frac{\partial}{\partial V_i} f_1 = J_{11}[f_1, f_1] + J_{12}[f_1, f_2], \tag{23}$$

$$-a_{ij}V_j \frac{\partial}{\partial V_i} f_2 = J_{22}[f_2, f_2] + J_{21}[f_2, f_1]. \tag{24}$$

The total pressure tensor is $\mathsf{P} = \mathsf{P}_1 + \mathsf{P}_2$, where the partial pressure tensors P_r ($r = 1, 2$) are defined by Eq. (19). The elements of these tensors can be obtained by multiplying the Boltzmann equations (23) and (24) by $m_r\mathbf{VV}$ and integrating over $\mathbf{V}$. The result is

$$a_{ik}P_{1,kj} + a_{jk}P_{1,ki} + B_{11}P_{1,ij} + B_{12}P_{2,ij} = (A_{11}\,p_1 + A_{12}\,p_2)\,\delta_{ij}, \tag{25}$$

where use has been made of Eq. (18) (with $\mathbf{j}_r = \mathbf{0}$) and I have introduced the coefficients

$$A_{11} = \frac{w_{11}}{2(d+2)}(1+\alpha_{11})^2 + \frac{w_{12}}{d+2}\mu_{21}^2(1+\alpha_{12})^2, \tag{26}$$

$$A_{12} = \frac{w_{12}}{d+2}\frac{\rho_1}{\rho_2}\mu_{21}^2(1+\alpha_{12})^2, \tag{27}$$

$$B_{11}=\frac{w_{11}}{d(d+2)}(1+\alpha_{11})(d+1-\alpha_{11})$$
$$+\frac{2w_{12}}{d(d+2)}\mu_{21}(1+\alpha_{12})[d+2-\mu_{21}(1+\alpha_{12})], \tag{28}$$

$$B_{12}=-\frac{2}{d}A_{12}. \tag{29}$$

A similar equation can be obtained for P_2, by just making the changes $1\leftrightarrow 2$. From Eq. (25), in particular, one gets

$$aP_{1,xy}=-\frac{d}{2}p_1\zeta_1. \tag{30}$$

In order to have explicit expressions one still needs to fix the parameters w_{rs}. The most natural choice to find good agreement with the IHS results is to adjust the cooling rates ζ_{rs} for IMM, Eq. (20), to be the same as those obtained for IHS. Given that the cooling rates for IHS are not exaclty known in the simple shear flow problem, I will take for ζ_{rs} the cooling rate of IHS evaluated at the first Sonine approximation:[28, 29]

$$\zeta_{rs}^{\text{IHS}}\to\frac{2\Omega_d}{\sqrt{\pi}\,d}n_s\mu_{sr}\sigma_{sr}^{d-1}v_0\left(\frac{\theta_r+\theta_s}{\theta_r\theta_s}\right)^{1/2}(1+\alpha_{rs})\left[1-\frac{\mu_{sr}}{2}(1+\alpha_{rs})\frac{\theta_r+\theta_s}{\theta_s}\right], \tag{31}$$

where $\sigma_{rs}=(\sigma_r+\sigma_s)/2$ and $v_0=\sqrt{2T(m_1+m_2)/m_1m_2}$ is a thermal velocity defined in tems of the granular temperature of the mixture T. Therefore, according to Eq. (20), the collision frequencies w_{rs} of IMM are given by

$$w_{rs}=\frac{\Omega_d}{\sqrt{\pi}}n_s\sigma_{rs}^{d-1}v_0\left(\frac{\theta_r+\theta_s}{\theta_r\theta_s}\right)^{1/2}, \tag{32}$$

where use has been made of the fact that $\mathbf{j}_r=\mathbf{0}$ in the simple shear flow state. Henceforth, I will present the results of IMM with this choice.

Equation (25) along with its counterpart for P_2 constitute a linear system of equations for the total pressure tensor P. In order to express the solution of this system, it is convenient to introduce dimensionless quantities. As done in a previous study for IHS,[28] I reduce the shear rate a with respect to an effective collision frequency

$$\nu=\frac{\Omega_d}{2\sqrt{\pi}}n\sigma_{12}^{d-1}v_0. \tag{33}$$

Thus, I introduce the reduced cooling rates $\zeta_r^* = \zeta_r/\nu$, the reduced shear rate $a^* = a/\nu$, and the reduced partial pressure tensors $\mathsf{P}_r^* = \mathsf{P}_r/x_r p$. The reduced total pressure tensor is $\mathsf{P}^* = \mathsf{P}/p = x_1\mathsf{P}_1^* + x_2\mathsf{P}_2^*$. It is worthwhile remarking that, for given values of the parameters of the mixture, a^* and P^* are *only* functions of the restitution coefficients α_{11}, α_{22}, and α_{12}.

In reduced units, the solution to Eq. (25) gives the pressure tensor P^* in terms of a^*, the temperature ratio γ, the restitution coefficients and the parameters of the mixture. The dependence of a^* on α_{rs} can be obtained from the energy equation (22) as

$$a^* = -\frac{d}{2}\frac{\zeta^*}{P_{xy}^*} = -\frac{d}{2}\frac{x_1\gamma_1\zeta_1^* + x_2\gamma_2\zeta_2^*}{x_1 P_{1,xy}^* + x_2 P_{2,xy}^*}, \tag{34}$$

where I have introduced the temperature ratios $\gamma_1 = T_1/T = (\mu_{21}\theta_1)^{-1}$ and $\gamma_2 = T_2/T = (\mu_{12}\theta_2)^{-1}$. When the dependence of P_r^* and a^* on the temperature ratio γ is known, the latter can be obtained by solving Eq. (30) (or its counterpart for the species 2)

$$\gamma = \frac{\zeta_2^* P_{1,xy}^*}{\zeta_1^* P_{2,xy}^*}. \tag{35}$$

Once Eq. (35) is solved, one gets the rheological properties (as measured by the elements of the pressure tensor) of the mixture in terms of the parameters of the problem. In the elastic limit ($\alpha_{11} = \alpha_{22} = \alpha_{22} = 1$), the cooling rate $\zeta = 0$ and the temperature increases in time due to viscous heating ($aP_{xy} \neq 0$). Consequently, for long times, the reduced shear rate $a^*(t) = a/\nu(t)$ tends to zero and one recovers the equilibrium results, $P_{ij}^* = \delta_{ij}$. Beyond the elastic limit, the reduced pressure tensor has a complex dependence on the restitution coefficients and the parameters of the mixture. Before considering the general case, let us study separately some interesting limit cases.

3.1. Mechanically Equivalent Particles

This simple case corresponds to $m_1 = m_2$, $\sigma_1 = \sigma_2$, and $\alpha_{11} = \alpha_{22} = \alpha_{12} \equiv \alpha$. In this limit, Eqs. (25), (34), and (35) yield $\gamma = 1$, $\mathsf{P}_1^* = \mathsf{P}_2^* = \mathsf{P}^*$, and the nonzero elements of the (reduced) pressure tensor can be written as

$$P_{yy}^* = P_{zz}^* = \cdots = P_{dd}^* = \frac{d}{2}\frac{1+\alpha}{d+1-\alpha}, \tag{36}$$

$$P_{xy}^* = -\sqrt{\frac{d^2(d+2)(1-\alpha^2)}{8(d+1-\alpha)^2}}, \tag{37}$$

$$P_{xx}^* = d-(d-1)\,P_{yy}^*. \tag{38}$$

Expressions (36)–(38) are independent of the choice of the collision frequency $w_{rs} \equiv w$.

Recently, Cercignani[25] has analyzed the simple shear flow problem of a monocomponent granular gas considering the more refined version of the Maxwell model indicated in Section 2. The results obtained by Cercignani[25] in the (steady) shear flow problem for a three dimensional system leads to the absence of the normal stress differences ($P^*_{xx} = P^*_{yy} = P^*_{zz} = 1$) and the shear stress is given by

$$P^*_{xy} = -\sqrt{3\frac{1-\alpha}{3-\alpha}}. \tag{39}$$

The elements of the pressure tensor of IHS have been explicitly obtained from the Boltzmann equation in the first Sonine approximation.[28, 29] For the sake of completeness, their expressions are displayed in Appendix B [cf. Eqs. (B5)–(B7)]. It is apparent that these expressions differ from those found here, Eqs. (36)–(38). However, for practical purposes, the discrepancies between both interaction models are quite small, even for moderate values of α. As an illustration, Fig. 1 shows a comparison of the results obtained for IMM and IHS for the (reduced) elements of the pressure tensor for $d = 3$. The results (symbols) obtained from Monte Carlo simulations for IHS[28] as well as the predictions for the shear stress given by Eq. (39) are also included. It can be observed that the discrepancies between IHS and IMM are very small, although they slightly increase

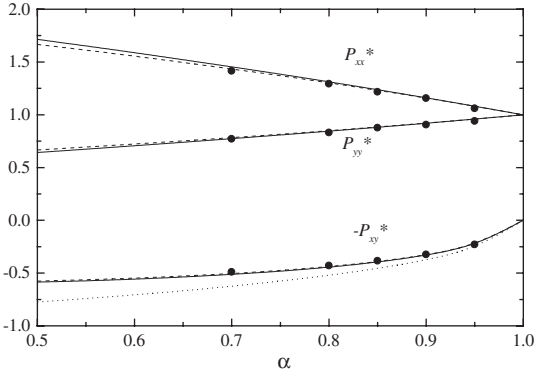

Fig. 1. Plot of the reduced elements of the pressure tensor P^* as functions of the restitution coefficient for a three-dimensional single gas. The solid lines are the results derived here for IMM, the dashed lines correspond to the results obtained for IHS from the Sonine approximation, and the symbols refer to Monte Carlo simulations for IHS.[28] The dotted line is the result given by Eq. (39).

as the restitution coefficient decreases. In addition, the agreement of both interaction models with simulation data is quite good. On the other hand, the results derived in ref. 25 exhibit significant discrepancies with Monte Carlo results, except in the low-dissipation region. These discrepancies could be due to the different version of IMM studied in ref. 25 or perhaps, to the (uncontrolled) approximations used there to obtain the pressure tensor in the steady state. Elucidation of this point requires further analysis.

3.2. Tracer Limit

When one of the species, say species 1, has a vanishing mole fraction, it acts as a tracer species. In this case, the state of the excess component 2 is not affected by the presence of the tracer particles and so the expression of P_2^* is the same as the one obtained in the single gas case, Eqs. (36)–(38), with $\alpha = \alpha_{22}$. The corresponding expressions for the elements of the tracer pressure tensor P_1^* can be obtained from Eq. (25) by taking carefully the limit $x_1 \to 0$. After some algebra, one gets

$$P_{1,yy}^* = P_{1,zz}^* = \cdots = P_{1,dd}^* = -\frac{F + HP_{2,yy}^*}{G}, \tag{40}$$

$$P_{1,xy}^* = \frac{a^* P_{1,yy}^* - HP_{2,xy}^*}{G}, \tag{41}$$

$$P_{1,xx}^* = d\gamma - (d-1)\, P_{1,yy}^*, \tag{42}$$

where

$$F = \frac{2}{d+2}\mu_{12}^{3/2}\mu_{21}\left(\frac{1+\theta}{\theta}\right)^{3/2}(1+\alpha_{12})^2, \tag{43}$$

$$G = \frac{4}{d(d+2)}\sqrt{\mu_{12}}\,\mu_{21}\left(\frac{1+\theta}{\theta}\right)^{1/2}(1+\alpha_{12})[\mu_{21}(1+\alpha_{12}) - d - 2], \tag{44}$$

$$H = \frac{4}{d(d+2)}\mu_{12}^{3/2}\mu_{21}\left(\frac{1+\theta}{\theta}\right)^{1/2}(1+\alpha_{12})^2, \tag{45}$$

and the reduced shear rate is

$$a^{*2} = \left(\frac{\sigma_2}{\sigma_{12}}\right)^{2(d-1)} \frac{2(d+1-\alpha_{22})^2\,(1-\alpha_{22}^2)}{d^2(d+2)}. \tag{46}$$

Here, $\theta = m_1 T_2 / m_2 T_1$ is the mean square velocity of the gas particles relative to that of the tracer particles. The temperature ratio γ is obtained from

Eq. (35) where the (reduced) cooling rates ζ_2^* and ζ_1^* in the tracer limit are given by

$$\zeta_2^* = \frac{\sqrt{2\mu_{12}}}{d}\left(\frac{\sigma_2}{\sigma_{12}}\right)^{d-1}(1-\alpha_{22}^2), \tag{47}$$

$$\zeta_1^* = \frac{4}{d}\mu_{21}\sqrt{\mu_{12}}\left(\frac{1+\theta}{\theta}\right)^{1/2}(1+\alpha_{12})\left[1-\frac{\mu_{21}}{2}(1+\theta)(1+\alpha_{12})\right]. \tag{48}$$

3.3. General Case: Comparison with IHS Results

Here, I compare the results obtained for IMM with those found for IHS by using the leading Sonine approximation[28] as well as by performing Monte Carlo simulations.[28, 30] Specifically, I want to explore the dependence of the temperature ratio γ and the nonzero elements of P^* on the restitution coefficients α_{rs}, the mass ratio m_1/m_2, the concentration ratio n_1/n_2, and the ratio of sizes σ_1/σ_2. Given the high dimensionality of the parameter space, for the sake of concreteness, henceforth I will assume that the disks or spheres are made of the same material, i.e., $\alpha_{11}=\alpha_{22}=\alpha_{12}\equiv\alpha$. This reduces the parameter space to four quantities.

The temperature ratio $\gamma = T_1/T_2$ measures the breakdown of energy equipartition. Due to the coupling between dissipation and the shear rate in the (steady) simple shear flow state [cf. Eq. (34)], the mixture departures from the Navier–Stokes regime as the restitution coefficient α decreases. Thus, energy nonequipartition is expected except when $\alpha\to 1$. The coexistence of two granular temperatures has been recently confirmed by molecular dynamics simulations carried out in sheared granular mixtures of hard disks[32] and by some experiments[33] of vibrated granular mixtures. Related findings have been reported by some authors by using kinetic theory tools in the freely cooling state for IHS[34, 35] and IMM.[26, 27] As expected, the results obtained here show that in general the kinetic temperatures of the mixture are different ($\gamma\neq 1$). The dependence of γ on the parameters of the problem is very complex. In Fig. 2 the temperature ratio T_1/T_2 is plotted versus the restitution coefficient α for an equimolar mixture ($n_1=n_2$) of hard spheres ($d=3$) with $\sigma_1/\sigma_2=1$ and two different values of the mass ratio: $m_1/m_2=2$ and 10. It can be clearly seen that the predictions for IMM agree quite well with the ones obtained for IHS in the first Sonine approximation and that the agreement of both approaches with simulation is excellent, even for moderate dissipation. It is also apparent that the extent of the equipartition violation is greater when the mass disparity is large. To illustrate this point, in Fig. 3, I consider an equimolar mixture of hard disks ($d=2$) of constant density, i.e., $m_1/m_2=(\sigma_1/\sigma_2)^2$.

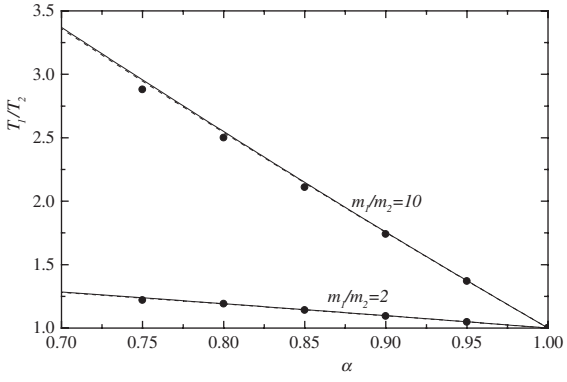

Fig. 2. Plot of the temperature ratio T_1/T_2 versus the restitution coefficient in the three-dimensional case for $n_1/n_2 = 1$, $\sigma_1/\sigma_2 = 1$, and two different values of the mass ratio m_1/m_2: $m_1/m_2 = 2$ and $m_1/m_2 = 10$. The solid lines are the results derived for IMM, the dashed lines correspond to the results obtained for IHS from the Sonine approximation, and the symbols refer to Monte Carlo simulations for IHS.[28]

Three different values of the restitution coefficient have been studied: $\alpha = 0.95$, 0.9, and 0.8. Again, the IMM results reproduce quite well the IHS predictions (theory and simulation) over the entire range of values of size and mass ratios considered. Further, the behavior of T_1/T_2 obtained here for dilute systems is qualitatively similar to that found in molecular dynamics simulations[32] for finite-density systems. Thus, for instance, at a

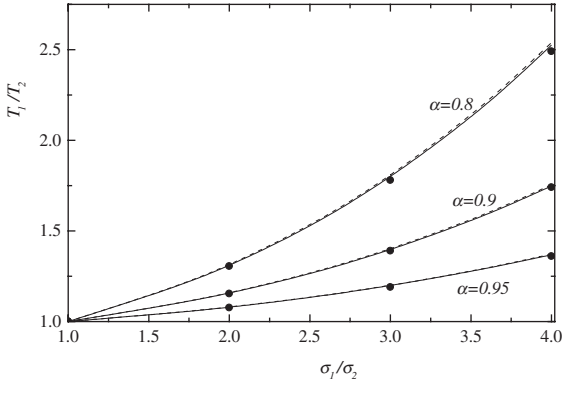

Fig. 3. Plot of the temperature ratio T_1/T_2 as a function of the size ratio $\sigma_1/\sigma_2 = (m_1/m_2)^{1/2}$ in the two-dimensional case for $n_1/n_2 = 1$ and three different values of the restitution coefficient α: $\alpha = 0.95$, $\alpha = 0.9$, and $\alpha = 0.8$. The solid lines are the results derived for IMM, the dashed lines correspond to the results obtained for IHS from the Sonine approximation, and the symbols refer to Monte Carlo simulations for IHS.[30]

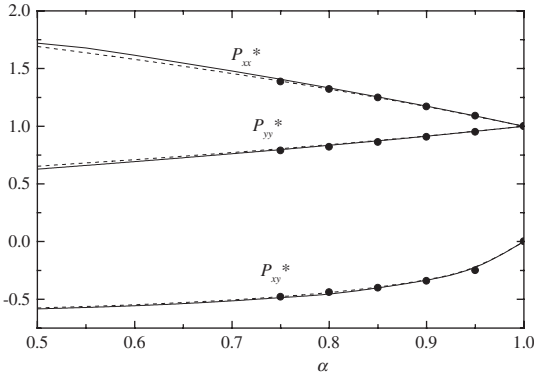

Fig. 4. Plot of the reduced elements of the pressure tensor P^* as functions of the restitution coefficient in the three-dimensional case for $n_1/n_2 = 1$, $\sigma_1/\sigma_2 = 1$, and $m_1/m_2 = 2$. The solid lines are the results derived for IMM, the dashed lines correspond to the results obtained for IHS from the Sonine approximation, and the symbols refer to Monte Carlo simulations for IHS.[28]

given value of α, the granular energy of the larger particle (say for instance, species 1) increases relative to that of the smaller particle as the ratio σ_1/σ_2 (or equivalently, m_1/m_2) increases.

The dependence of the nonzero elements of the pressure tensor P^* on the restitution coefficient α is illustrated in Figs. 4 and 5 for two different mixtures. In Fig. 4, I consider a mixture of hard spheres ($d = 3$) with

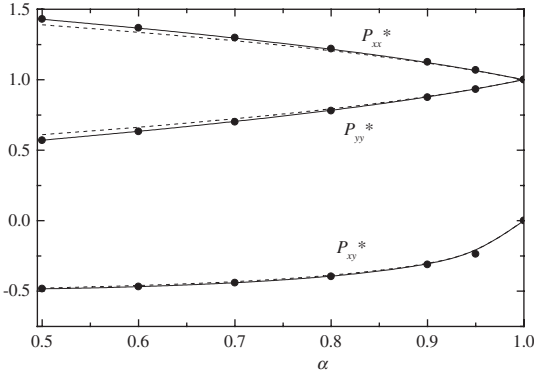

Fig. 5. Plot of the reduced elements of the pressure tensor P^* as functions of the restitution coefficient α in the two-dimensional case for $n_1/n_2 = 1$ and $\sigma_1/\sigma_2 = (m_1/m_2)^{1/2} = 10$. The solid lines are the results derived for IMM, the dashed lines correspond to the results obtained for IHS from the Sonine approximation, and the symbols refer to Monte Carlo simulations for IHS.[28]

$n_1/n_2 = \sigma_1/\sigma_2 = 1$ and $m_1/m_2 = 2$, while Fig. 5 corresponds to a mixture of hard disks ($d = 2$) with $n_1/n_2 = 1$, $m_1/m_2 = (\sigma_1/\sigma_2)^2 = 10$. It is apparent that the agreement between the results derived for IMM and IHS is again in general quite good, especially in the case of the shear stress P^*_{xy} which is the most relevant rheological property in a shear flow problem. In fact, in the two-dimensional case, the exact results obtained here for IMM are closer to the simulation results than those obtained by using the first Sonine approximation for IHS.[28] It must be remarked that both theories only predict normal stress differences in the plane of shear flow ($P^*_{xx} > P^*_{yy} = P^*_{zz} = \cdots = P^*_{dd}$), while the simulation results also show anisotropy in the plane orthogonal to the flow velocity ($P^*_{zz} > P^*_{yy}$). However, these relative normal stress differences are very small and tend to zero as the restitution coefficient decreases.

4. DIFFUSION OF IMPURITIES UNDER GRANULAR SHEAR FLOW

The second problem analyzed in this paper refers to the diffusion of impurities in a granular Maxwell gas subjected to the simple shear flow. This problem has also been recently analyzed by the author[29] in the framework of IHS. In the tracer limit ($x_1 \to 0$), the state of the excess component is not affected by the presence of the tracer particles so that its velocity distribution function f_2 verifies a closed Boltzmann equation. As a consequence, the pressure tensor P^*_2 of the granular gas is given by Eqs. (36)–(38). Further, given that the mole fraction of the tracer particles x_1 is very small, one can neglect their mutual interactions in the kinetic equation for f_1 and assume that f_1 verifies a (linear) Boltzmann–Lorentz equation. The diffusion process is induced in the system by the presence of a *weak* concentration gradient ∇x_1. Given that the strength of the shear rate a is arbitrary, the mass flux $\mathbf{j}_1$ (which is generated by the gradient ∇x_1) can be modified by the presence of the shear flow. Under these conditions, a diffusion tensor D is required to describe the diffusion process instead of a single diffusion coefficient. The determination of the nonzero elements of this tensor is the goal of this section.

In the local Lagrangian frame, the kinetic equation governing the evolution of the velocity distribution function f_1 reads

$$\frac{\partial}{\partial t} f_1 - a_{ij} V_j \frac{\partial}{\partial V_i} f_1 + (V_i + a_{ij} r_j) \frac{\partial}{\partial r_i} f_1 = J_{12}[\mathbf{V} \mid f_1, f_2], \tag{49}$$

where here the spatial derivative $\partial f_1/\partial r_i$ is taken at constant $\mathbf{V}$. Assuming that the mole fraction x_1 is slightly *nonuniform*, I solve Eq. (49) by means

of a perturbation expansion around a nonequilibrium state with arbitrary shear rate. Thus, I write

$$f_1 = f_1^{(0)} + f_1^{(1)} + \cdots, \tag{50}$$

where $f_1^{(k)}$ is of order k in ∇x_1 but applies for *arbitrary* degree of dissipation since this distribution retains all the orders in a^*. The solution (50) qualifies as a normal solution since all the space and time dependence of f_1 occurs entirely through $x_1(\mathbf{r}; t)$ and their gradients. The zeroth-order approximation $f_1^{(0)}$ corresponds to the simple shear flow distribution but taking into account now the local dependence on the mole fraction x_1. Although the explicit form of $f_1^{(0)}$ is not exactly known, only the knowledge of its second-degree moments is necessary to get the diffusion tensor. The explicit expressions of the (reduced) pressure tensor P_1^* are given by Eqs. (40)–(45).

The kinetic equation for $f_1^{(1)}$ can be obtained from the Boltzmann–Lorentz equation (49) by collecting all the terms of first order in ∇x_1:

$$\frac{\partial}{\partial t} f_1^{(0)} - a_{ij} V_j \frac{\partial}{\partial V_i} f_1^{(1)} + (V_i + a_{ij} r_j) \frac{\partial}{\partial r_i} f_1^{(0)} = J_{12}[\mathbf{V} \mid f_1^{(1)}, f_2]. \tag{51}$$

The determination of the diffusion tensor from Eq. (51) follows similar mathematical steps as those made in the case of IHS. I refer the reader to ref. 29 for more specific details and here only some intermediate results will be displayed. Using the balance equation for the mass density of impurities, Eq. (51) becomes

$$\left(a_{ij} V_j \frac{\partial}{\partial V_i} + \Lambda \right) f_1^{(1)} = \frac{\partial f_1^{(0)}}{\partial x_1} (\mathbf{V} \cdot \nabla x_1), \tag{52}$$

where Λ is the Boltzmann–Lorentz collision operator

$$\Lambda f_1^{(1)} = J_{12}[\mathbf{V} \mid f_1^{(1)}, f_2]. \tag{53}$$

The mass flux $\mathbf{j}_1^{(1)}$ is defined as

$$\mathbf{j}_1^{(1)} = m_1 \int d\mathbf{v}\, \mathbf{V} f_1^{(1)}. \tag{54}$$

The components of $\mathbf{j}_1^{(1)}$ can be obtained by multiplying Eq. (52) by $m_1 \mathbf{V}$ and integrating over $\mathbf{V}$. The result can be written as

$$(\mathsf{a} + \lambda \mathbb{1}) \cdot \mathbf{j}_1^{(1)} = -p_2 \mathsf{P}_1^* \cdot \nabla x_1, \tag{55}$$

where use has been made of Eq. (17) (with $\mathbf{j}_2 = \mathbf{0}$) and $\mathbb{1}$ is the $d \times d$ unit tensor. The coefficient λ is

$$\lambda = \frac{w_{12}}{d} \mu_{21}(1+\alpha_{12})$$
$$= \frac{2}{d} \frac{\pi^{(d-1)/2}}{\Gamma(d/2)} n_2 \mu_{21} \sigma_{12}^{d-1} (2T_2/m_2)^{1/2} (1+\alpha_{12}) \left(\frac{1+\theta}{\theta} \right)^{1/2}. \tag{56}$$

Note that, according to Eq. (20), w_{12} is still given by Eq. (32) since $\mathbf{j}_2 = \mathbf{0}$. The solution to Eq. (55) can be written in the form

$$\mathbf{j}_1^{(1)} = -\mathsf{D} \cdot \nabla x_1, \tag{57}$$

with the elements of the diffusion tensor D given by

$$D_{ij} = \frac{p_2}{\lambda} \left(\delta_{ik} - \frac{a_{ik}}{\lambda} \right) P^*_{1,kj}. \tag{58}$$

Equation (58) provides an explicit expression of the tracer diffusion tensor of a granular Maxwell mixture under shear flow. In the absence of shear rate ($a = 0$), as well as in the elastic limit ($\alpha_{22} = \alpha_{12} = 1$), one has $D_{ij} = D_0 \delta_{ij}$, where

$$D_0 = \frac{d}{4\sqrt{2}} \frac{\Gamma(d/2)}{\pi^{(d-1)/2} \sigma_{12}^{d-1}} \sqrt{\frac{m_1(m_1+m_2)}{m_2} T_2} \tag{59}$$

is the tracer diffusion coefficient of a gas of Maxwell molecules.[36] As the restitution coefficient decreases, rheological effects become important and the elements of the diffusion tensor are different from the one obtained in the equilibrium case. The dependence of the diffusion coefficients on the restitution coefficients α_{22} and α_{12} as well as on the mass ratio m_1/m_2 and the size ratio σ_1/σ_2 is highly nonlinear. As happens for elastic fluids,[37] Eq. (58) shows that diffusion under simple shear flow is a very complex problem due basically to the anisotropy induced in the system by the shear flow.

To illustrate the dependence of the elements of the diffusion tensor on the parameters of the problem, let us consider the three dimensional case ($d = 3$). According to Eq. (58), $D_{xz} = D_{zx} = D_{yz} = D_{zy} = 0$, in agreement with the symmetry of the problem. Consequently, there are five relevant elements: the three diagonal and two (D_{xy}, D_{yx}) off-diagonal elements. In general, $D_{xx} \neq D_{yy} = D_{zz}$ and $D_{xy} \neq D_{yx}$. The off-diagonal elements are negative and measure cross effects in the diffusion of impurities in a sheared granular gas. The results obtained[29] for IHS [cf. Eqs. (B8)–(B13)

of Appendix B] also predict anisotropy in the plane perpendicular to the shear flow ($D_{yy} \neq D_{zz}$), although this anisotropy is much smaller than the one observed in the plane of shear flow (as measured by the difference $D_{xx} - D_{yy}$). In Fig. 6, the self-diffusion problem is considered, i.e., when the tracer particles are mechanically equivalent to the gas particles. This figure shows $D^*_{xx} - D^*_{yy}$, $(D^*_{xx} + D^*_{yy} + D^*_{zz})/3 \equiv (1/3)\, D^*_{kk}$, D^*_{xy}, and D^*_{yx} as functions of the restitution coefficient $\alpha \equiv \alpha_{12} = \alpha_{22}$. Here, $D^*_{ij} \equiv D_{ij}/D_0$, with D_0 given by Eq. (59). It can be seen that the deviation from the functional form for elastic collisions is quite important even for moderate dissipation. The figure also shows that the anisotropy of the system, as measured by the difference $D^*_{xx} - D^*_{yy}$ grows with the inelasticity. It is worthwhile remarking that the general qualitative behavior of the self-diffusion tensor on dissipation agrees well with molecular dynamics simulations carried out by Campbell,[38] at least for the lowest solid fraction considered in his simulations. With respect to the comparison with the results for IHS,[29] we see again good agreement although the discrepancies between both interaction models slightly increase as α decreases. In fact, these discrepancies are more significant than those found for the rheological properties in the simple shear flow problem. Finally, Fig. 7 shows the dependence of D^*_{ij} on α in the case $m_1/m_2 = 2$ and $\sigma_1/\sigma_2 = 2$ for IMM and IHS. Similar conclusions to those made in the self-diffusion case are obtained here for mixtures of species with different (but not disparate) mass and size. It must be pointed out that the discrepancies for the diffusion tensor between both interaction models turn out to be significant as the disparity of masses or sizes increases.

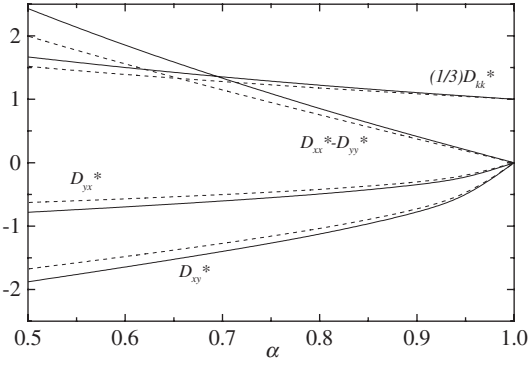

Fig. 6. Dependence of the diagonal and off-diagonal elements of the reduced self-diffusion tensor D^* on the restitution coefficient α in the three-dimensional case. The solid lines are the results derived for IMM while the dashed lines correspond to the results obtained for IHS from the Sonine approximation.

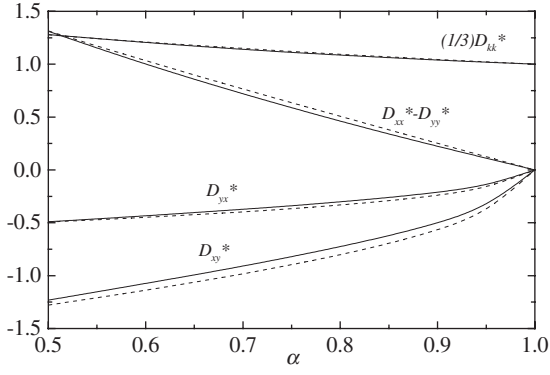

Fig. 7. Dependence of the diagonal and off-diagonal elements of the reduced diffusion tensor D^* on the restitution coefficient α in the three-dimensional case for $\sigma_1/\sigma_2 = 1$ and $m_1/m_2 = 2$. The solid lines are the results derived for IMM while the dashed lines correspond to the results obtained for IHS from the Sonine approximation.

5. CONCLUDING REMARKS

Needless to say, the analysis of nonlinear transport phenomena (i.e., when the hydrodynamic gradients are not necessarilly small) from the Boltzmann equation for inelastic hard spheres (IHS) is a formidable task. For this reason, to get explicit results one usually considers the leading order in a Sonine polynomial expansion of the velocity distribution function. All the above difficulties increase when one studies polydisperse systems (granular mixtures) since not only is the number of transport coefficients larger than for a monomponent gas but they are also functions of more parameters such as the concentrations, masses, sizes, and the coefficients of restitution. A possible way to partially overcome these problems is to consider interaction models (such as the inelastic Maxwell model) that simplify the mathematical structure of the Boltzmann collision operator. For elastic fluids, this strategy has been shown to be very fruitful since the exact results[10, 11] obtained for Maxwell molecules for many interesting transport properties (both linear and nonlinear) agrees quite well with hard spheres and other interaction potentials when they are convenienlty nondimensionalized.[12]

In the Boltzmann equation for inelastic Maxwell models (IMM), the collision rate of IHS is replaced by an effective collision rate independent of the two colliding particles. The simplicity of this interaction model allows us for instance, to get exactly the moments of the Boltzmann collision operator without the explicit knowledge of the velocity distribution function. The cost of sacrificing physical realism can be compensated by

the amount of exact analytical results obtained from IMM. However, in order to assess the degree of usefulness of IMM as a prototype model for the description of granular media, one needs to compare the predictions based on IMM with those obtained in the framework of the IHS model. In this paper I have carried out such a comparison at the level of nonlinear transport in two different but related nonequilibrium problems. First, I have explicitly determined the rheological properties (pressure tensor) of a binary inelastic Maxwell mixture under simple shear flow. Then, by taking the above solution as the reference state, I have obtained the diffusion tensor of impurities immersed in a sheared inelastic Maxwell gas. In the context of IMM, both expressions are exact in the sense that they apply for arbitrary values of the restitution coefficients and the parameters characterizing the mixture (masses, sizes, and concentrations).

Previous studies of such nonlinear transport coefficients have been carried out[28, 29] by the author in the case of IHS. As said above, these results[28, 29] are approximate since they are obtained by retaining the first terms in a Sonine polynomial expansion of the velocity distribution functions. However, the accuracy of these results[28, 29, 39] has been confirmed by Monte Carlo simulations[28, 30] of the Boltzmann equation. To compare the results derived from IMM and IHS, the collision frequencies w_{rs} appearing in the Boltzmann equation for IMM [see Eq. (2)] need to be fixed. Here, to make contact with IHS, I have chosen w_{rs} to reproduce the cooling rates ζ_{rs} of IHS. With this choice, the results derived here for IMM for the pressure tensor and the diffusion tensor compare quite well with the ones previously derived for IHS over a wide range of values of dissipation and parameters of the mixture. Given the high dimensionality of the parameter space explored, the comparison carried out in this paper can be considered as a good test to gauge the reliability of IMM to reproduce the main trends observed for IHS in the context of granular mixtures.

Finally, it must be noted that the good agreement found here contrasts with the results recently derived for the Navier–Stokes (NS) transport coefficients,[23] where it was shown that the dependence of the transport coefficients of IMM on the restitution coefficient only compares well at a qualitatively level with the one obtained for IHS. However, the situation analyzed in ref. 23 is completely different to the one studied here since the Navier–Stokes coefficients were obtained in the first order of the Chapman–Enskog expansion around a time-dependent state (homogeneous cooling state). In this sense, it seems that the results found in this paper for IMM may be sufficiently representative of the trends observed for IHS in some particular situations (such as the simple shear flow problem), and this agreement must be taken with caution when one explores other situations. This fact stimulates the search for exact solutions for IMM which can be

confronted with the results obtained for IHS by using approximate analytical methods and computer simulations.

APPENDIX A. COLLISIONAL MOMENTS IN THE INELASTIC MAXWELL MODEL

In this appendix I will derive the collisional moments appearing in the main text. Let us consider the general collisional integral

$$I_{rs}[F] = \int d\mathbf{v}\, F(\mathbf{V})\, J_{rs}[f_r, f_s]. \tag{A1}$$

A useful identity for an arbitrary function $F(\mathbf{V})$ is given by

$$I_{rs}[F] = \frac{w_{rs}}{n_s \Omega_d} \int d\mathbf{v}_1 \int d\mathbf{v}_2\, f_r(\mathbf{V}_1)\, f_s(\mathbf{V}_2) \int d\hat{\boldsymbol{\sigma}} [F(\mathbf{V}_1'') - F(\mathbf{V}_1)], \tag{A2}$$

with

$$\mathbf{V}_1'' = \mathbf{V}_1 - \mu_{sr}(1+\alpha_{rs})(\hat{\boldsymbol{\sigma}} \cdot \mathbf{g}_{12})\, \hat{\boldsymbol{\sigma}}, \tag{A3}$$

and $\mathbf{g}_{12} = \mathbf{V}_1 - \mathbf{V}_2$. Now I particularize to $F(\mathbf{V}) = m_r \mathbf{V}$. Using (A2), one gets

$$I_{rs}[m_r \mathbf{V}] = -\frac{w_{rs}}{n_s \Omega_d} m_r \mu_{sr}(1+\alpha_{rs}) \int d\mathbf{v}_1 \int d\mathbf{v}_2\, f_r(\mathbf{V}_1)\, f_s(\mathbf{V}_2) \int d\hat{\boldsymbol{\sigma}} (\hat{\boldsymbol{\sigma}} \cdot \mathbf{g}_{12})\, \hat{\boldsymbol{\sigma}}. \tag{A4}$$

To perform the angular integration, one needs the result[17]

$$\int d\hat{\boldsymbol{\sigma}} (\hat{\boldsymbol{\sigma}} \cdot \mathbf{g}_{12})^k\, \hat{\boldsymbol{\sigma}} = \beta_{k+1} g_{12}^{k-1} \mathbf{g}_{12}, \tag{A5}$$

where

$$\beta_k = \Omega_d \pi^{-1/2} \frac{\Gamma(\frac{d}{2})\, \Gamma(\frac{k+1}{2})}{\Gamma(\frac{k+d}{2})}. \tag{A6}$$

Thus, the integration over $\hat{\boldsymbol{\sigma}}$ in Eq. (A4) leads to

$$\begin{aligned} I_{rs}[m_r \mathbf{V}] &= -\frac{w_{rs}}{n_s d} m_r \mu_{sr}(1+\alpha_{rs}) \int d\mathbf{v}_1 \int d\mathbf{v}_2\, f_r(\mathbf{V}_1)\, f_s(\mathbf{V}_2)(\mathbf{V}_1 - \mathbf{V}_2) \\ &= -\frac{w_{rs}}{\rho_s d} \mu_{sr}(1+\alpha_{rs})(\rho_s \mathbf{j}_r - \rho_r \mathbf{j}_s), \end{aligned} \tag{A7}$$

where $\rho_r = m_r n_r$ and

$$\mathbf{j}_r = \int d\mathbf{v}\, m_r \mathbf{V} f_r(\mathbf{v}). \tag{A8}$$

Next, I particularize to $F(\mathbf{V}) = m_r \mathbf{V}\mathbf{V}$. From the collision rule (A3) it follows that

$$\mathbf{V}_1''\mathbf{V}_1'' - \mathbf{V}_1\mathbf{V}_1 = \mu_{sr}(1+\alpha_{rs})(\hat{\boldsymbol{\sigma}}\cdot\mathbf{g}_{12})[\mu_{sr}(1+\alpha_{rs})(\hat{\boldsymbol{\sigma}}\cdot\mathbf{g}_{12})\,\hat{\boldsymbol{\sigma}}\hat{\boldsymbol{\sigma}} - (\mathbf{V}_1\hat{\boldsymbol{\sigma}} + \hat{\boldsymbol{\sigma}}\mathbf{V}_1)]. \tag{A9}$$

To perform the angular integration in (A7), I need now the result

$$\int d\hat{\boldsymbol{\sigma}}(\hat{\boldsymbol{\sigma}}\cdot\mathbf{g}_{12})^k\,\hat{\boldsymbol{\sigma}}\hat{\boldsymbol{\sigma}} = \frac{\beta_k}{k+d}\, g_{12}^{k-2}(k\mathbf{g}_{12}\mathbf{g}_{12} + g_{12}^2\mathbb{1}), \tag{A10}$$

where $\mathbb{1}$ is the $d\times d$ unit tensor. By using the identity (A2) and Eqs. (A9) and (A10), the collisional moment $I_{rs}[m_r\mathbf{V}\mathbf{V}]$ can be finally written as

$$\begin{aligned} I_{rs}[m_r\mathbf{V}\mathbf{V}] &= \frac{w_{rs}}{n_s d} m_r \mu_{sr}(1+\alpha_{rs}) \int d\mathbf{V}_1 \int d\mathbf{V}_2\, f_r(\mathbf{V}_1)\, f_s(\mathbf{V}_2) \\ &\quad \times \left[\frac{\mu_{sr}(1+\alpha_{rs})}{d+2}(2\mathbf{g}_{12}\mathbf{g}_{12} + g_{12}^2\mathbb{1}) - (\mathbf{V}_1\mathbf{g}_{12} + \mathbf{g}_{12}\mathbf{V}_1)\right] \\ &= -\frac{w_{rs}}{\rho_s d}\mu_{sr}(1+\alpha_{rs})\Big\{2\rho_s\mathsf{P}_r - (\mathbf{j}_r\mathbf{j}_s + \mathbf{j}_s\mathbf{j}_r) \\ &\quad -\frac{2}{d+2}\mu_{sr}(1+\alpha_{rs})\Big[\rho_s\mathsf{P}_r + \rho_r\mathsf{P}_s - (\mathbf{j}_r\mathbf{j}_s + \mathbf{j}_s\mathbf{j}_r) \\ &\quad + \left[\frac{d}{2}(\rho_r p_s + \rho_s p_r) - \mathbf{j}_r\cdot\mathbf{j}_s\right]\mathbb{1}\Big]\Big\}. \end{aligned} \tag{A11}$$

Here, $p_r = \mathrm{Tr}\,\mathsf{P}_r/d = n_r T_r$ with

$$\mathsf{P}_r = \int d\mathbf{v}\, m_r \mathbf{V}\mathbf{V} f_r(\mathbf{v}). \tag{A12}$$

In the simple shear flow state, $\mathbf{j}_r = \mathbf{0}$, and the expression (A11) for the collisional moment $I_{rs}[m_r\mathbf{V}\mathbf{V}]$ becomes

$$\begin{aligned} I_{rs}[m_r\mathbf{V}\mathbf{V}] &= \frac{2}{d+2}\frac{w_{rs}}{\rho_s d}\mu_{sr}^2(1+\alpha_{rs})^2 \\ &\quad \times\left[\left(1 - \frac{d+2}{\mu_{sr}(1+\alpha_{rs})}\right)\rho_s\mathsf{P}_r + \rho_r\mathsf{P}_s + \frac{d}{2}(\rho_r p_s + \rho_s p_r)\,\mathbb{1}\right]. \end{aligned} \tag{A13}$$

From Eq. (A13) one can easily get the coefficients A_{rs} and B_{rs} appearing in Eqs. (26)–(29). In the case of mechanically equivalent particles ($m_1 = m_2 = m$, $\sigma_1 = \sigma_2 = \sigma$, $\alpha_{11} = \alpha_{22} = \alpha_{12} = \alpha$), one has $T_1 = T_2 = T$, $\mathsf{P}_1 = \mathsf{P}_2 = \mathsf{P}$, and so the collisional moment $I_{rs}[m_r \mathbf{VV}] \equiv I[m\mathbf{VV}]$ reduces to

$$I[m\mathbf{VV}] = \frac{1}{2(d+2)} w(1+\alpha)\left[(1+\alpha)\, p\, \mathbb{1} - \frac{2}{d}(d+1-\alpha)\, \mathsf{P} \right]. \tag{A14}$$

This expression coincides with the one previously derived in the monocomponent case.[23]

APPENDIX B. SOME EXPRESSIONS FOR INELASTIC HARD SPHERES

The shear flow problem for a binary mixture of IHS was studied in refs. 28 and 29. I give here some expressions obtained for this interaction model in the first Sonine approximation that have been used along the paper to compare them with the results derived for IMM.

For IHS the expressions of the coefficients A_{11}, A_{21}, B_{11}, and B_{12} appearing in Eqs. (25) are given by

$$A_{11} = \frac{\sqrt{2}}{d(d+2)} x_1 \left(\frac{\sigma_1}{\sigma_{12}}\right)^{d-1} \theta_1^{-1/2}(1+\alpha_{11})[\alpha_{11}(d-1)+d+1]\, \nu, \tag{B1}$$

$$A_{12} = \frac{2}{d(d+2)} x_1 \mu_{12} \theta_2^{-1/2} \left(\frac{\theta_1+\theta_2}{\theta_1}\right)^{3/2} (1+\alpha_{12}) \times \left[\frac{2\theta_2}{\theta_1+\theta_2} + \mu_{21}(d-1)(1+\alpha_{12}) \right] \nu, \tag{B2}$$

$$B_{11} = \frac{\sqrt{2}}{d(d+2)} x_1 \left(\frac{\sigma_1}{\sigma_{12}}\right)^{d-1} \mu_{21}\theta_1^{1/2}(1+\alpha_{11})(2d+3-3\alpha_{11})\, \nu + \frac{2}{d(d+2)} x_2 \mu_{21}^2 \left(\frac{\theta_1}{\theta_2(\theta_1+\theta_2)}\right)^{1/2} \times \{[2d-3\mu_{21}(1+\alpha_{12})](\theta_1+\theta_2) + 2(2\theta_1+3\theta_2)\}\, \nu, \tag{B3}$$

$$B_{12} = -\frac{2}{d(d+2)} x_1 \mu_{12}^2 \left(\frac{\theta_2^3}{\theta_1(\theta_1+\theta_2)}\right)^{1/2} \left[3\mu_{21} \frac{\theta_1+\theta_2}{\theta_2}(1+\alpha_{12}) - 2 \right] \nu. \tag{B4}$$

Here, θ_1 and θ_2 are defined by Eq. (21) while ν is the effective collision frequency defined by Eq. (33). From Eqs. (B1)–(B4) and their counterpart for species 2, the temperature ratio and the elements of the pressure tensor

can be easily obtained. In the special case of mechanically equivalent particles, Eqs. (B1)–(B4) lead to the following expressions for the nonzero elements of the reduced presure tensor P^*:

$$P_{yy}^* = P_{zz}^* = \cdots = P_{dd}^* = \frac{d+1+(d-1)\,\alpha}{2d+3-3\alpha}, \tag{B5}$$

$$P_{xy}^* = -\sqrt{\frac{d(d+2)[d+1+(d-1)\,\alpha](1-\alpha)}{2(2d+3-3\alpha)^2}}, \tag{B6}$$

$$P_{xx}^* = d-(d-1)\,P_{yy}^*. \tag{B7}$$

Tracer diffusion under shear flow was analyzed in ref. 29 for IHS. The expression of the diffusion tensor is

$$\mathsf{D} = p_2(\mathsf{a}+\boldsymbol{\Omega})^{-1}\cdot\mathsf{P}_1^*, \tag{B8}$$

where the tensor $\boldsymbol{\Omega}$ is

$$\boldsymbol{\Omega} = \lambda\left[\mathbb{1}+\frac{1}{d+2}\frac{\theta}{1+\theta}(\mathsf{P}_2^*-\mathbb{1})\right]. \tag{B9}$$

Here, λ is given by Eq. (56) and the pressure tensor P_2^* of the excess component is given by Eqs. (B5)–(B7). The nonzero elements of P_1^* can be written in the form given by Eqs. (40)–(42) but the functions F, G, and H are

$$F = \frac{4}{d(d+2)}\mu_{12}^{3/2}\left(\frac{1+\theta}{\theta^3}\right)^{1/2}(1+\alpha_{12})\left[1+\frac{\mu_{21}}{2}(d-1)(1+\theta)(1+\alpha_{12})\right], \tag{B10}$$

$$G = -\frac{2}{d(d+2)}\sqrt{\mu_{12}}\,\mu_{21}\left(\frac{1}{\theta(1+\theta)}\right)^{1/2}(1+\alpha_{12}) \times\{2[(d+2)\,\theta+d+3]-3\mu_{21}(1+\theta)(1+\alpha_{12})\}, \tag{B11}$$

$$H = \frac{2}{d(d+2)}\mu_{12}^{3/2}\left(\frac{1}{\theta(1+\theta)}\right)^{1/2}(1+\alpha_{12})[3\mu_{21}(1+\theta)(1+\alpha_{12})-2], \tag{B12}$$

and the reduced shear rate is

$$a^{*2} = \left(\frac{\sigma_2}{\sigma_{12}}\right)^{2(d-1)}\frac{\mu_{12}}{d(d+2)}\frac{(1+\alpha_{22})(2d+3-3\alpha_{22})^2\,(1-\alpha_{22}^2)}{d+1+(d-1)\,\alpha_{22}}. \tag{B13}$$

ACKNOWLEDGMENTS

Partial support from the Ministerio de Ciencia y Tecnología (Spain) through Grant No. BFM2001-0718 is acknowledged.

REFERENCES

1. J. J. Brey, J. W. Dufty, and A. Santos, Dissipative dynamics for hard spheres, *J. Stat. Phys.* **87**:1051–1066 (1997); T. P. C. van Noije, M. H. Ernst, and R. Brito, Ring kinetic theory for an idealized granular gas, *Physica A* **251**:266–283 (1998).
2. J. J. Brey, J. W. Dufty, C. S. Kim, and A. Santos, Hydrodynamics for granular flow at low density, *Phys. Rev. E* **58**:4638–4653 (1998).
3. V. Garzó and J. W. Dufty, Dense fluid transport for inelastic hard spheres, *Phys. Rev. E* **59**:5895–5911 (1999).
4. V. Garzó and J. M. Montanero, Transport coefficients of a heated granular gas, *Physica A* **313**:336–356 (2002).
5. V. Garzó and J. W. Dufty, Hydrodynamics for a granular mixture at low density, *Phys. Fluids* **14**:1476–1490 (2002).
6. J. Lutsko, J. J. Brey, and J. W. Dufty, Diffusion in a granular fluid. II. Simulation, *Phys. Rev. E* **65**:051304 (2002).
7. J. J. Brey, M. J. Ruiz-Montero, and D. Cubero, On the validity of linear hydrdodynamics for low-density granular flows described by the Boltzmann equation, *Europhys. Lett.* **48**:359–364 (1999).
8. J. M. Montanero and V. Garzó, Shear viscosity for a heated granular binary mixture at low-density, *Phys. Rev. E* **67**:021308 (2003).
9. M. H. Ernst, Non-linear model-Boltzmann equations and exact solutions, *Phys. Rep.* **78**: 1–171 (1981).
10. C. Truesdell, On the pressures and the flux of energy in a gas according to Maxwell's kinetic theory, II, *J. Rat. Mech. Anal.* **5**:55-128 (1956).
11. C. Truesdell and R. G. Muncaster, *Fundamentals of Maxwell's Kinetic Theory of a Simple Monatomic Gas* (Academic Press, New York, 1980).
12. A. Santos and V. Garzó, Exact non-linear transport from the Boltzmann equation, in *Rarefied Gas Dynamics 19*, J. Harvey and G. Lord, eds. (Oxford University Press, Oxford, 1995), pp. 13–22.
13. W. Loose and S. Hess, Velocity distribution function of a streaming gas via nonequilibrium molecular dynamics, *Phys. Rev. Lett.* **58**:2443–2445 (1987); W. Loose, The constant-temperature constraint in the nonequilibrium molecular dynamics and the non-Newtonian viscosity coefficient of gases, *Phys. Lett. A* **128**:39–44; J. Gómez Ordoñez, J. J. Brey, and A. Santos, Shear-rate dependence of the viscosity for dilute gases, *Phys. Rev. A* **39**: 3038–3040 (1989).
14. E. Ben-Naim and P. L. Krapivsky, Multiscaling in inelastic collisions, *Phys. Rev. E* **61**: R5–R8 (2000).
15. A. V. Bobylev, J. A. Carrillo, and I. M. Gamba, On some properties of kinetic and hydrodynamic equations for inelastic interactions, *J. Stat. Phys.* **98**:743–773 (2000).
16. J. A. Carrillo, C. Cercignani, and I. M. Gamba, Steady states of a Boltzmann equation for driven granular media, *Phys. Rev. E* **62**:7700–7707 (2000).
17. M. H. Ernst and R. Brito, Scaling solutions of inelastic Boltzmann equations with over-populated high energy tails, *J. Stat. Phys.* **109**:407–432 (2002).

18. A. Baldasarri, U. M. B. Marconi, and A. Puglisi, Influence of correlations of the velocity statistics of scalar granular gases, *Europhys. Lett.* **58**:14–20 (2002).
19. P. L. Krapivsky and E. Ben-Naim, Scaling, multiscaling, and nontrivial exponents in inelastic collision processes, *Phys. Rev. E* **66**:011309 (2002).
20. M. H. Ernst and R. Brito, Driven inelastic Maxwell models with high energy tails, *Phys. Rev. E* **65**:040301(R) (2002).
21. A. V. Bobylev and C. Cercignani, Self-similar asymptotics for the Boltzmann equation with inelastic and elastic interactions, *J. Stat. Phys.* **110**:333–375 (2003).
22. A. V. Bobylev, C. Cercignani, and G. Toscani, Proof of an asymptotic property of self-similar solutions of the Boltzmann equation for granular materials, *J. Stat. Phys.* **111**: 403–416 (2003).
23. A. Santos, Transport coefficients of *d*-dimensional inelastic Maxwell models, *Physica A* **321**:442–466 (2003).
24. H. Hayakawa, Hydrodynamics for inelastic Maxwell model, cond-mat/0209630.
25. C. Cercignani, Shear flow of a granular fluid, *J. Stat. Phys.* **102**:1407–1415 (2001).
26. U. M. B. Marconi and A. Puglisi, Mean-field model of free-cooling inelastic mixtures, *Phys. Rev. E* **65**:051305 (2002); Steady state properties of a mean field model of driven inelastic mixtures, *Phys. Rev. E* **66**:011301 (2002).
27. E. Ben-Naim and P. L. Krapivsky, Impurity in a granular fluid, *Eur. Phys. J. E* **8**:507–515 (2002).
28. J. M. Montanero and V. Garzó, Rheological properties in a low-density granular mixture, *Phys. A* **310**:17–38 (2002).
29. V. Garzó, Tracer diffusion in granular shear flows, *Phys. Rev. E* **66**:021308 (2002).
30. J. M. Montanero and V. Garzó, Energy nonequipartition in a sheared granular mixture, *Mol. Sim.* (to be published) and cond-mat/0204205.
31. A. V. Bobylev and C. Cercignani, Moment equations for a granular material in a thermal bath, *J. Stat. Phys.* **106**:547–567 (2002).
32. R. Clelland and C. Hrenya, Simulations of a binary-sized mixture of inelastic grains in rapid shear flow, *Phys. Rev. E* **65**:031301 (2002).
33. R. D. Wildman and D. J. Parker, Coexistence of two granular temperatures in binary vibrofluidized beds, *Phys. Rev. Lett.* **88**:064301 (2002); K. Feitosa and N. Menon, Breakdown of energy equipartition in a 2D binary vibrated granular gas, *Phys. Rev. Lett.* **88**: 198301 (2002).
34. V. Garzó and J. W. Dufty, Homogeneous cooling state for a granular mixture, *Phys. Rev. E* **60**:5706–5713 (1999); J. M. Montanero and V. Garzó, Monte Carlo simulation of the homogeneous cooling state for a granular mixture, *Granular Matter* **4**:17–24 (2002).
35. J. W. Dufty and V. Garzó, Mobility and diffusion in granular fluids, *J. Stat. Phys.* **105**: 723–744 (2001).
36. S. Chapman and T. G. Cowling, *The Mathematical Theory of Nonuniform Gases* (Cambridge University Press, Cambridge, 1970).
37. V. Garzó, A. Santos, and J. J. Brey, Influence of nonconservative external forces on self-diffusion in dilute gases. *Physica A* **163**:651–671 (1990); V. Garzó and M. López de Haro, Tracer diffusion in shear flow, *Phys. Rev. A* **44**:1397–1400 (1991); Kinetic models for uniform shear flow, *Phys. Fluids A* **4**:1057–1069 (1992); C. Marín and V. Garzó, Mutual diffusion in a binary mixture under shear flow, *Phys. Rev. E* **57**:507–513 (1998).
38. C. S. Campbell, Self-diffusion in granular shear flows, *J. Fluid Mech.* **348**:85–101) (1997).
39. A. V. Bobylev, M. Groppi, and G. Spiga, Approximate solutions to the problem of stationary shear flow of granular material, *Eur. J. Mech. B Fluids* **21**:91 103 (2002).